JOURNAL OF WATER AND LAND DEVELOPMENT
e-ISSN 2083-4535
Polish Academy of Sciences (PAN) Institute of Technology and Life Sciences – National Research Institute (ITP – PIB)

JOURNAL OF WATER AND LAND DEVELOPMENT
DOI: 10.24425/jwld.2024.151791
2024, No. 63 (X-XII): 67–77

Mangrove degradation and fish pond expansion analysis in North Kalimantan, Indonesia, using automatic maps of mangroves and shorelines indices

Suyarso* ✉, Praditya Avianto ✉

National Research and Innovation Agency, Research Center for Oceanography, Jl. Pasir Putih 1, Ancol Timur, 14430, Jakarta, Indonesia

* Corresponding author

RECEIVED 24.10.2023 ACCEPTED 09.08.2024 AVAILABLE ONLINE 02.12.2024

Abstract: The east coast of North Kalimantan Province, Indonesia, from the northern border with Sabah, Malaysia, to the south, consists of a series of estuarine landscapes in the north and a delta in the south. Landsat imagery acquired in 1995 shows that there are 150,869 ha of pristine mangrove forest and 14,456 ha of ponds. The mangrove mapping uses the automatic mangrove map and index (*AMMI*). For ponds mapping, we have introduced the automatic shoreline map (*ASM*) index, automatic mapping of water body including the shoreline, ponds and rivers.

Landsat image from 2000 shows that the mangrove area has decreased to 100,016 ha, while the pond area increased to 27,903 ha. Landsat image from 2010 shows that the mangrove area was 106,867 ha, while the pond area increased to 74,270.2 ha. Landsat imagery from 2022 shows that the remaining mangrove area was 108,187 ha, while the pond area increased further to 84,182 ha.

Mangrove decline was extreme from 1995 to 2000, coinciding with Indonesia's currency crisis. Currency devaluation encouraged local communities and entrepreneurs to create export commodities, with shrimp exports being one of the most promising. To maintain the presence of mangroves, the government implemented a silvo-fishery policy, while farming, it was also restoring mangroves. This paper introduces the fusion of two indices that automatically map mangrove environments to inform multi-temporal changes of mangroves, ponds, and shorelines based on Landsat imagery more accurately, faster, and with lower cost and labour.

Keywords: mangrove changes, fish ponds expansion, currency crisis, automatic mangrove map and index, automatic shoreline map

INTRODUCTION

The transportation of sediments by large rivers and their subsequent deposition in the sea usually leads to the creation of new intertidal land and facilitates the growth of mangroves (Long *et al.*, 2022). These plants are of paramount importance to all living organisms, from the simplest microorganisms and plants to the most complex living systems, and they have considerable economic potential in terms of natural resources (Costanza *et al.*, 1997; Nagelkerken *et al.*, 2008). Numerous shrimp ponds have been established in or near mangroves and tidal channels because they are suitable for brackish water and shrimp farming (Wang *et al.*, 2010). Mangroves are coastal plants that thrive in tropical and subtropical regions in the intertidal zone. These ecosystems are known for their biodiversity and serve as spawning and feeding grounds for various fish species (Donato *et al.*, 2011), as a habitat for wildlife on land, and as a temporary home for many migratory birds (Nagelkerken *et al.*, 2008).

Mangrove roots capture the accumulation of heavy metals and toxic organic substances in sediments in the presence of pollutants in the marine environment (Yam *et al.*, 2020), can clean sewage (Wong, Tam and Lan, 1997), prevent seawater intrusion (Kim *et al.*, 2016), and act as a barrier for coastal

protection and stabilisation (Danielsen *et al.*, 2005; Dahdouh-Guebas *et al.*, 2006; Das and Vincent, 2009).

In the context of climate change, mangrove ecosystems play an important role in carbon sequestration as they can absorb atmospheric carbon through photosynthesis and store it in the soil (Fatoyinbo *et al.*, 2008; Wang *et al.*, 2010; Wicaksono *et al.*, 2016; Sanderman *et al.*, 2018; Jones *et al.*, 2020).

Mangrove ecosystems respond to both anthropogenic and natural disturbances. The degradation of mangrove populations has been well-documented since the 1990s. Anthropogenic disturbances to mangrove degradation include conversion to aquaculture and agriculture (Thu and Populus, 2007; Veettil *et al.*, 2018), conversion of mangrove areas to commercial environments, including residential infrastructure and aquaculture facilities (Boon, 2001; Ng and Ong, 2022), urban expansion (Valiela, Bowen and York, 2001; Alongi, 2002; Duke *et al.*, 2007; Giri *et al.*, 2011; Kanniah *et al.*, 2015), and illegal logging for fuel and construction materials (Soemodihardjo, Suroyo and Suyarso, 1991). Of particular concern is the fact that in the 1990s and 2000s, mangrove areas were converted into fish ponds not only in Indonesia; this phenomenon is also occurring in neighbouring countries such as Vietnam (Hauser *et al.*, 2017; Alban de *et al.*, 2020), Thailand (Macintosh, Ashtona and Havanon, 2002), China (Chen *et al.*, 2009), Mexico (Adame *et al.*, 2018), and such regions as Southeast Asia and Asia-Pacific (Gandhi and Jones, 2019). Natural disturbances that threaten mangroves include cyclones, tsunamis and earthquakes that cause coastal land uplift (Ross *et al.*, 2006; Taylor, Rangel-Salazar and Hernández, 2013).

The Indonesian aquaculture industry alone is responsible for around a quarter of the mangrove loss in Southeast Asia since 2000 (Richards and Friess, 2015).

Currently, the global focus is on climate change and the physical occurrence of hazards, often referred to as hazards or climate risks (Brooks, 2003), and their impacts on sea level rise that have significant effects on coastal environments. Most mangroves cannot keep up with the rise in sea level because the sediments are not very high and the soil migration space is limited (Gilman *et al.*, 2008). Sierra-Correa and Cantera Kintz (2015) emphasise that in tropical countries where mangrove forests thrive, the long-term threat of sea level rise requires coastal planning to avoid much greater losses. Temporal satellite data using spectral indices from combinations of surface reflectances at different wavelengths can be used to analyse changes in the land surface over time. Therefore, remote sensing and GIS techniques provide detailed spatial and temporal information about objects on the Earth's surface. The Landsat satellites have long provided data that has been successfully used in many medium-scale environmental studies and there is almost no cost to users. Both satellites can cover a large area with a high temporal resolution, which makes them ideal for monitoring the ecosystem on a national scale (Giri *et al.*, 2011, Purnamasayangsukasih *et al.*, 2016; Guo *et al.*, 2018; Wang *et al.*, 2019).

Traditionally, maps for mangroves and ponds are created by visual interpretation using manual digitisation on a screen. However, this work is tedious and time-consuming (Kuenzer *et al.*, 2011), and its quality depends on the interpreter (Thakur *et al.*, 2020). Currently, the rate of mangrove encroachment is faster than that of data collection and mangrove mapping. Rapid and accurate mapping of mangrove forests is urgently needed to provide information on the current status and changes in mangrove forests, and to promote better management in the future.

The study area is the east coast of the North Kalimantan Province, which borders the state of Sabah, Malaysia (Fig. 1). Based on Landsat 5 TM imagery acquired in 1995, the area consisted mainly of 150,869 ha of mangroves and 14,456 ha of ponds. However, based on Landsat 8 OLI imagery acquired in 2022, the area has been converted into ponds and only a few mangrove forests remain. In this study, an automatic mangrove detection index is used and an automatic water index is proposed to accurately map mangroves, ponds, rivers and coastlines using Landsat 5 thematic mapper (TM), Landsat 7 enhanced thematic mapper (ETM), and Landsat 8 operational land imager (OLI) imagery. This paper introduces the fusion of two indices that automatically map mangrove environments to inform multi-temporal changes in mangrove forests, ponds and shorelines more accurately, faster, and at lower cost based on multi-temporal Landsat imageries. This method particularly will be useful for stakeholders, communities and the private sector in monitoring, preserving and managing mangrove forests against pond expansion and shoreline erosion/accretion.

Fig. 1. The study area on the east coast of North Kalimantan Province, Indonesia (in the north, bordered by the state of Sabah, Malaysia); source: own elaboration based on BIG (2017)

MATERIALS AND METHODS

MATERIALS

The primary data used for the study were level-2 surface reflectance of Landsat 5 thematic mapper (TM) informed land cover in 1995, Landsat 7 enhanced thematic mapper (ETM) informed land cover in 2000 and 2010, and Landsat 8 operational land imager (OLI) informed land cover in 2022 which can be downloaded from the United States Geological Survey (USGS, no date) using the Google Earth Engine (GEE) facility. The GEE facility provides users with access to an extensive satellite imagery dataset and enormous computing capabilities (Gorelick *et al.*, 2017). The GEE feature helps download cloud-free satellite image data in cloudy areas, although the image coverage is based on a time-domain range. In areas that are often cloudy, data collection requires a longer coverage time range. In general, it takes approximately one year for the GEE setup to obtain a completely cloud-free image. The images used in this study of mangrove changes in North Kalimantan are listed in Table 1, and

Table 1. Imageries used in the study

Satellite imagery	Date of record	Resolution (m)	Cloud cover (%)	Damage (%)
Landsat 5 TM	January 1 – December 31, 1995	30	7	2
Landsat 7 ETM	January 1 – December 31, 2000	30	5	2
Landsat 7 ETM	January 1 – December 31, 2010	30	3	7
Landsat 8 OLI	January 1 – December 31, 2022	30	3	0

Explanations: TM = thematic mapper, ETM = enhanced thematic mapper, OLI = operational land imager.
Source: own elaboration based on USGS (no date).

band designation and sensor characteristics of Landsat 5 TM, Landsat 7 ETM, and Landsat 8 OLI imageries are shown in Table 2.

Table 2. Band designation and sensor characteristics in Landsat 5 TM, Landsat 7 ETM, and Landsat 8 OLI imageries

Landsat 5 TM	Landsat 7 ETM	Landsat 8 OLI	Resolution (m)	Wave length (μm)	Description
band					
1	1	2	30	0.450–0.515	blue
2	2	3	30	0.525–0.600	green
3	3	4	30	0.630–0.680	red
4	4	5	30	0.845–0.885	NIR
5	5	6	30	1.560–1.660	SWIR1
7	7	7	30	2.100–2.300	SWIR2

Explanations: NIR = near infra-red, SWIR1 = short wave infra-red 1, SWIR2 = short wave infra-red 2; TM, ETM, OLI as in Tab. 1.
Source: own elaboration based on USGS (no date).

METHODS

Water index and automatic shoreline map

The shoreline in this study was a temporary line in which there was a boundary line between the river water/seawater masses and land at the time of image acquisition, so it is very dynamic depending on the angle of the bottom of the water, the season and especially the tidal range. A wider application is to separate land and water, including ponds, rice fields, dams, shorelines and rivers.

Identification of water bodies using satellite images is traditionally performed using supervised classification, although this method is often hampered due to the similarity of the spectral characteristics between water and cloud shadows (Li *et al*., 2022). In recent years mapping of water bodies has also been done using an index based on spectral pairs corresponding to water features.

The modified normalised difference water index (*mNDWI*) was developed by Xu (2006) to modify the index of the normalised difference water index (*NDWI*) that was created by McFeeters (1996) due to certain limitations of the index using Landsat TM/ETM data. This approach not only rectifies the deficiencies and mitigates the weaknesses of *NDWI*, such as shadows and noise, but also enhances the informative content of the aquatic environment. Presently, it is widely acknowledged that *mNDWI* is more robust and dependable than *NDWI*, owing to the fact that the SWIR1 and SWIR2 bands are less susceptible to variations in sediment concentrations and other optically active constituents in water, as compared to the NIR band (Huang *et al*., 2018).

The new water index (*NWI*) is a water-extracting technique proposed by Ding (2009) that uses the four spectral reflectance bands of the Landsat 8 satellite: blue, NIR, SWIR1, and SWIR2 bands. This new index replaces the green band with blue and the NIR band with the total reflectance of the three infrared bands (NIR + SWIR1 + SWIR2).

The water ratio index (*WRI*) dewatering technique proposed by Shen and Li (2010) used the four spectral reflectance bands of the Landsat ETM satellite: green, red, NIR, and SWIR1 bands, because of the spectral characteristics of the water body: (green + red) > (NIR + SWIR1).

The water index (*WI*2015) was proposed by Fisher, Flood and Danaher (2016) and is based on reflectance values from Landsat ETM, which has been used to map land cover and wetlands in eastern Australia for more than 10 years. The *WI*2015 aims to improve upon the previous *WI*2006 by using five reflectances: green, red, NIR, SWIR1, SWIR2, and six empirical coefficients. The *WI*2015 has a theoretical range of –50 to 50, and 0 is the recommended threshold.

The multi band water index (*MBWI*) for the Landsat 8 OLI was published by Wang *et al.* (2018) and suggested maximising the spectral difference between water and non-water surfaces using green, NIR, SWIR1 and SWIR2 reflectance.

All existing water index and the formulas proposed by previous researchers are presented in Table 3.

Table 3. Summaries of the existing water indices and the equations

Water index	Equation	Reference
mNDWI	(green – SWIR1) / (green + SWIR1) + α	Xu (2006)
NWI	[blue – (NIR + SWIR1 + SWIR2)] / [blue + NIR + SWIR1 + SWIR2] + α	Ding (2009)
WRI	(green + red) / (NIR + SWIR2) + α	Shen and Li (2010)
*WI*2015	1.7204 + 171·green + 3·red – 70·NIR – 45·SWIR1 – 71·SWIR2 + α	Fisher, Flood and Danaher (2016)
MBWI	(2·green – red – NIR – SWIR1 – SWIR2) + α	Wang *et al.* (2018)

Explanations: α = gain constant, *mNDWI* = modified normalised difference water index, *NWI* = new water index, *WRI* = water ratio index, *WI*2015 = water index 2015, *MBWI* = multi band water index; SWIR1, SWIR2, NIR as in Tab. 2.
Source: own elaboration based on references in the Table.

The proposed for the new water index

In this study, we propose a new water index using a combination of SWIR1, NIR, and green reflectance, called the automatic shoreline map (*ASM*) index. The tryout result is shown in Fig. 2, the cropped image of Landsat 8 OLI was acquired in 2022 using RGB composite image of NIR–SWIR1–red bands with 30 m spatial resolution, and Fig. 2b shows the reflectance magnitude of each band along the A–B transect of Fig 2a. Ponds and dikes appear clearer/sharper at SWIR1, NIR, and green reflectance compared to blue or red reflectance. Significant differences between the three reflectance values provided much sharper results when separating waters, including shorelines, rivers, and ponds.

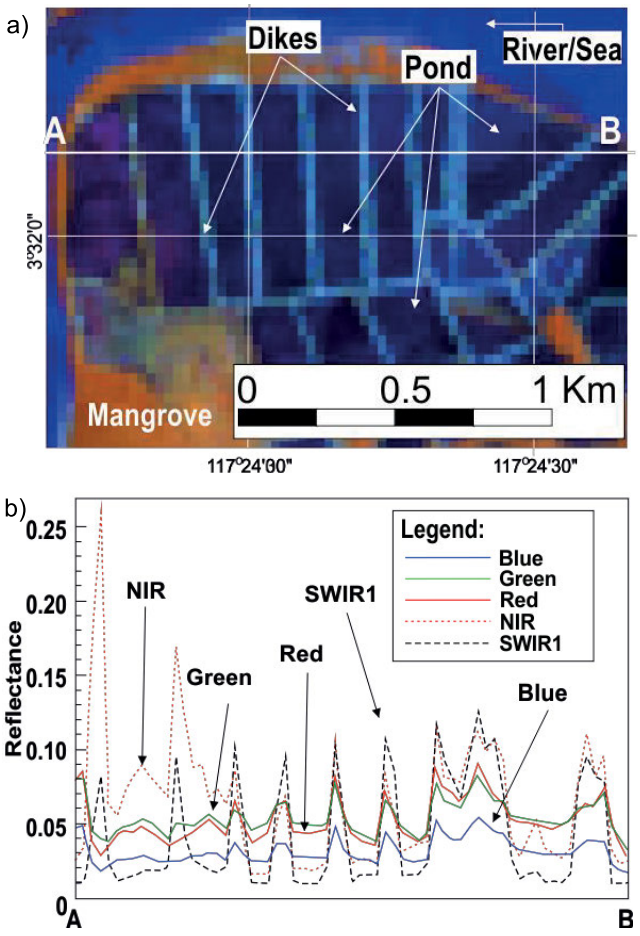

Fig. 2. Crop of Landsat 8 operational land imager (OLI): near infra-red (NIR) – short wave infra-red 1 (SWIR1) – red composite image acquired in 2022 showing the ponds and dikes, and A–B the transect line (a) reflectance magnitude of blue, green, red, NIR, and SWIR1 along the transect line A–B (b); source: own study

Based on Figure 2, it makes no sense that the dike width in ponds is generally less than 5 m, yet it is clearly visible on Landsat 8 imagery with a spatial resolution of 30 m. The physical properties of pond dikes, which are typically excavated of pond materials that have dried and opened, are believed to have an amplifying effect, reflecting more visible light and providing a visual contrast to water bodies that absorb more light. The proposed water index is formulated using three bands of satellite imagery:

$$ASM = \frac{\text{NIR} - \text{green/SWIR1}}{\text{NIR} + \text{SWIR1/green}} \quad (1)$$

Statistical verification of the index was performed by manually digitising the images, relying on the acuity of the eye in separating land (mangroves, pond dikes, shrubs) and water bodies (rivers, ponds, sea) on the island area. A total of 100 test points on land and in water were prepared and each index was run on Landsat imagery. The accuracy of the formulas is determined based on the plot of the test points on the image from the execution of each index. The percentage accuracy is determined based on the number of missing points and the number of correct points on the object.

Mangrove map

Automatic mangrove mapping was done using automatic mangrove map and index (*AMMI*) (Suyarso, 2022; Suyarso and Avianto, 2022), which uses a combination of red, NIR and SWIR1 reflectance. This index is capable of automatically mapping mangroves to separate them from other vegetation and provide excellent information on mangrove canopy density, formulated:

$$AMMI = \frac{\text{NIR} - \text{red}}{\text{red} + \text{SWIR1}} \cdot \frac{\text{NIR} - \text{SWIR1}}{\text{SWIR1} - 0.65 \cdot \text{red}} \quad (2)$$

The satellite image processing was conducted on the Google Earth Engine (GEE) platform to produce multi-temporal *AMMI* and *ASM* images. After all image data has been transformed into vector data, the reclassifying of rivers, ponds and seas is analysed using QGIS 3.16 software.

RESULTS AND DISCUSSIONS

PHYSICAL ENVIRONMENT

Geographically, the study area can be divided into two coastal landforms, namely the estuarine coast in the north and the deltaic coast in the south. The estuarine coast in the north is the mouth of the Sebuku River. The river is wide, but short, resembling only a bay. The connection to the open sea of the Sulawesi Sea is protected by the islands of Sebatik and Nunukan. In the south are the deltaic coast of the Sembakung, Sesayap and Kayan rivers. The Kayan River is the longest river (576 km) in North Kalimantan, which has its headwaters at Mount Ukeng and flowing into the Sulawesi Sea, forming the large delta of the Tanjung Selor delta complex (Fig. 3).

THE NEW WATER INDEX

In this study, the new water index is used to distinguish and separate water bodies (ponds, rivers, swamps and seas) from land. The author will not evaluate the performance of all existing water indices, but in general, some have shown satisfactory performance. In Figure 3a, the physical environment of the study area on the border with Malaysia is depicted. In Figure 3b, there is a small crop of a Landsat 2022 image of one of the islands without cloud cover with an RGB NIR–SWIR1–red composite image to show the sharp boundaries between land and water. The image was then digitised through screen digitising, which relies on the

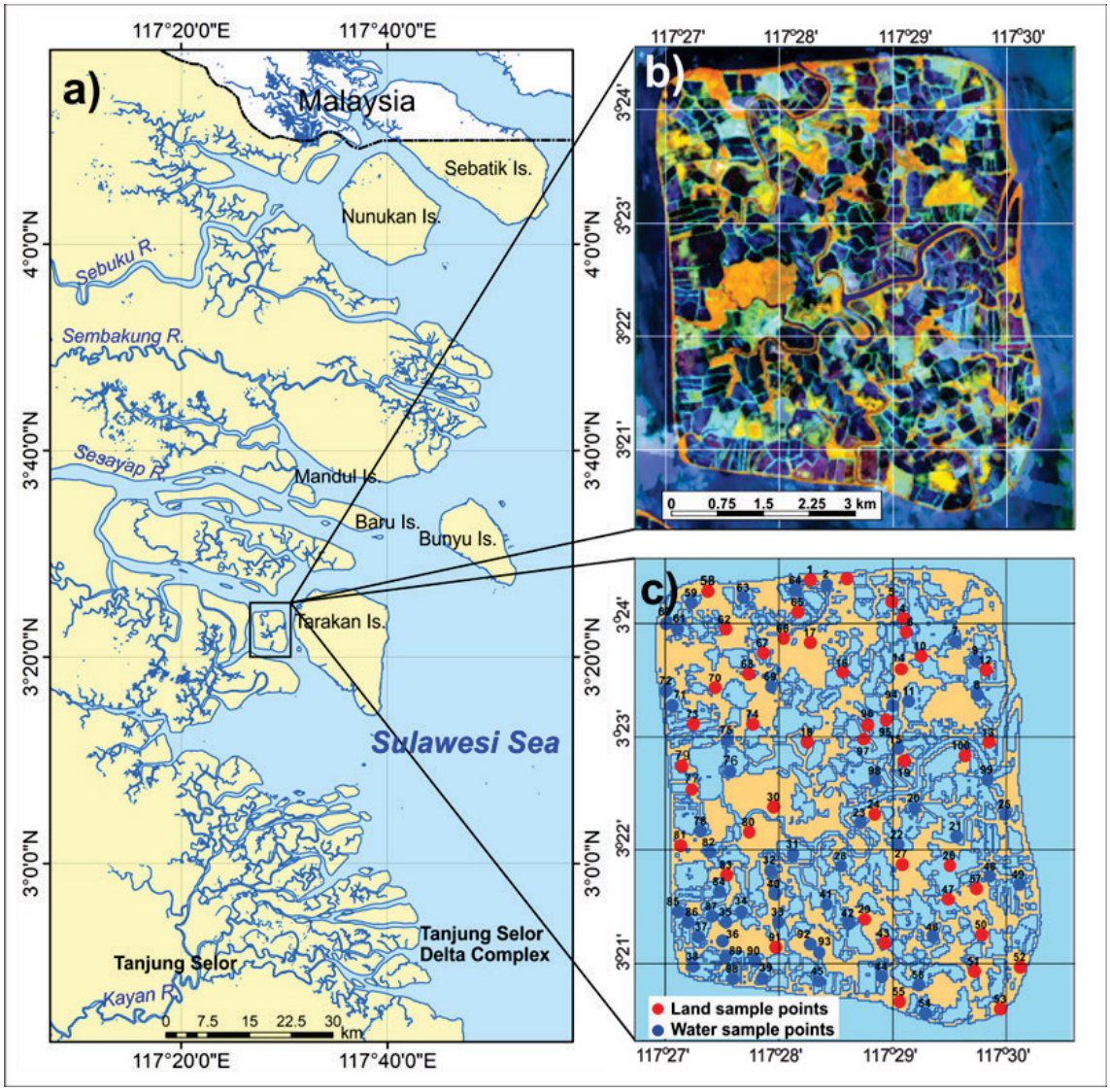

Fig. 3. Map of: a) physical environment of the study area, b) a crop of Landsat image from 2022 of one of the islands located between Tarakan Island (Is.) and the main land in near infra-red (NIR) – short wave infra-red 1 (SWIR1) – red composite image, c) map of ponds through manual digitising with 100 sample points representing water and land; source: own study based on Landsat imagery

sharpness of the eye. A total of 100 test points were prepared to test the accuracy (Fig. 3c), which were divided into points on land and points in water areas, especially ponds.

The performance in separation of mangrove, river and pond features in the study area through Landsat 8, 2022 image using the existing water index and *ASM* index is shown in Figure 4. One of the problems in using the existing water index is the setting of α (gain constant). The performance of some water index is indicated by α. If α is enlarged, wetlands and even pond dikes will disappear and become water objects, but if it is downsized, shallow waters become land objects. In calibration, in addition to field data, manual digitisation data that relies on eye sharpness is reliable data.

It can be seen that in Figure 4, the *ASM* index is quite sharp in separating land and water objects using three spectral reflectances with a fairly simple formula and with fairly good accuracy, as shown in Table 4. These findings provide a basis for optimism in the computation of the examined pond in the study area.

MANGROVE CHANGES AND PONDS GROWTH 1995–2022

The 1995 Landsat 5 TM imagery, which shows the condition of ponds and mangroves in 1995, was used as the starting point for the analysis of mangrove change in North Kalimantan because no older Landsat images were available. This year, ponds were only identified along the west coast of Tarakan Island and in the southern part of the Sesayap River Delta (Figs. 5 and 6). Meanwhile, in the Kayan River Delta, ponds were only identified in the northern part of the delta.

Analysis of mangrove conditions in 1995 showed extensive mangrove forests in some places, particularly in the northern area, the estuary west of Sebatik Island and Nunukan Island had a dense to moderate canopy index. On the other hand, in the south, particularly in the Kayan River Delta, the mangrove canopy index was generally moderate to low (Tab. 4 and Fig. 7). The total mangroves in the study area in 1995 reached 150,869 ha, while the identified ponds were 14,456 ha.

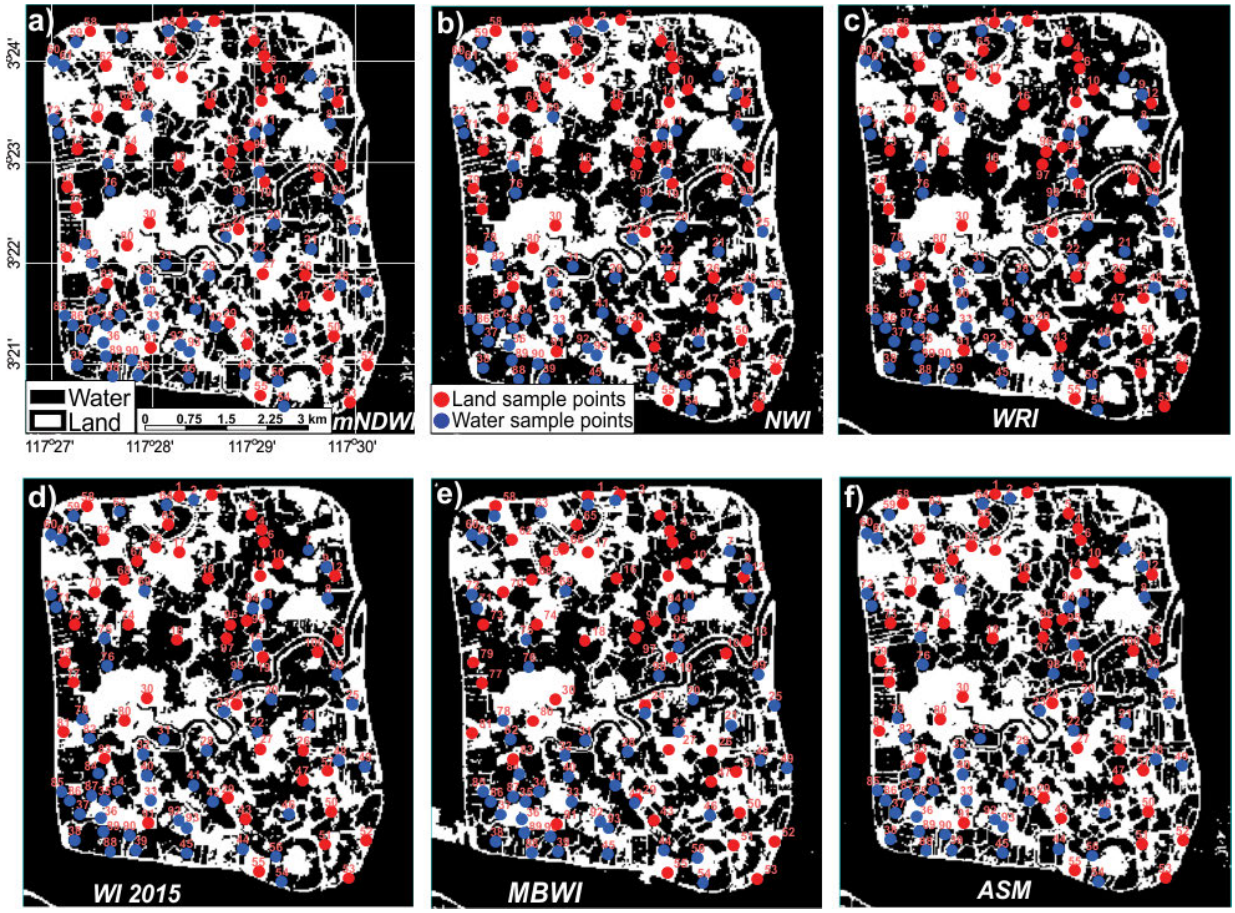

Fig. 4. Showing the performance of some water index on small island between Tarakan Island and the mainland: a) *mNDWI*, b) *NWI*, c) *WRI*, d) *WI*2015, e) automatic shoreline map (*ASM*) index; *mNDWI*, *NWI*, *WRI*, *WI*2015, *MBWI* as in Tab. 3; source: own study

The 2000 Landsat 7 ETM imagery indicates the status of ponds and mangroves in North Kalimantan in 2000. The northern mangrove area showed no change with a high to moderate canopy index and no ponds were identified on satellite imagery. New ponds were identified in the southern area, particularly in the south of Mandul Island and in the western part of Tarakan Island. These ponds were occupied on land that was formerly a mangrove habitat (Fig. 5). While several ponds were identified on the west coast of Tarakan Island in 1995, some had disappeared. The rapid changes of ponds in this area had resulted in the loss of most of the mangroves and only the banks and channels of the estuaries remained. In the Kayan River Delta area, especially in the northeastern part, ponds were growing quite rapidly and were located in the former mangrove habitat. Although ponds in the Kayan River Delta had only been identified in the northeast (Fig. 6), most of the mangrove habitat in the delta was beginning to disappear (Fig. 7). It is estimated that some of the ponds were operational in 2000 and others were in preparation. The mangrove area in 2000 was 100,016 ha, and ponds were recorded at 27,903 ha (Tab. 4).

The 2010 Landsat 7 ETM image provides information on the status of the ponds and mangroves in the study area in 2010. The ponds in the Sesayap River Delta area north of Tarakan Island have continued to show their westward changes and even the expansion of these ponds upstream of the Sesayap River (Fig. 5). These changes have resulted in the loss of most of the mangrove habitat. In the south, around the Kayan River Delta, ponds have taken up most of the delta area (Fig. 6). Interestingly, the identified mangrove area increased during this period. The pond, which was opened in 2000, is partly overgrown with mangroves with a high canopy index (Fig. 7). It is estimated that the operation of the ponds will be accompanied by the planting of mangroves in the surrounding land and abandoned ponds to protect the ponds from erosion. In the delta of the Kayan River environment, the mangrove area continues to increase, suggesting that mangrove planting around ponds is still ongoing (Fig. 8). The identified mangrove area was 106,867 ha and the pond area was 74,270.2 ha (Tab. 4).

Table 4. Performance and level of accuracy of each of the available water indices

Index	α	Missed point	Correct point	Accuracy (%)
mNDWI	0	2	98	98
NWI	–0.65	5	95	95
WRI	0.75	11	89	89
*WI*2015	–1.5	5	95	95
MBWI	–0.15	5	95	95
ASM	–1	2	98	98

Explanations: *ASM* = automatic shoreline map index, *α*, *mNDWI*, *NWI*, *WRI*, *WI*2015, *MBWI* as in Tab. 3.
Source: own study.

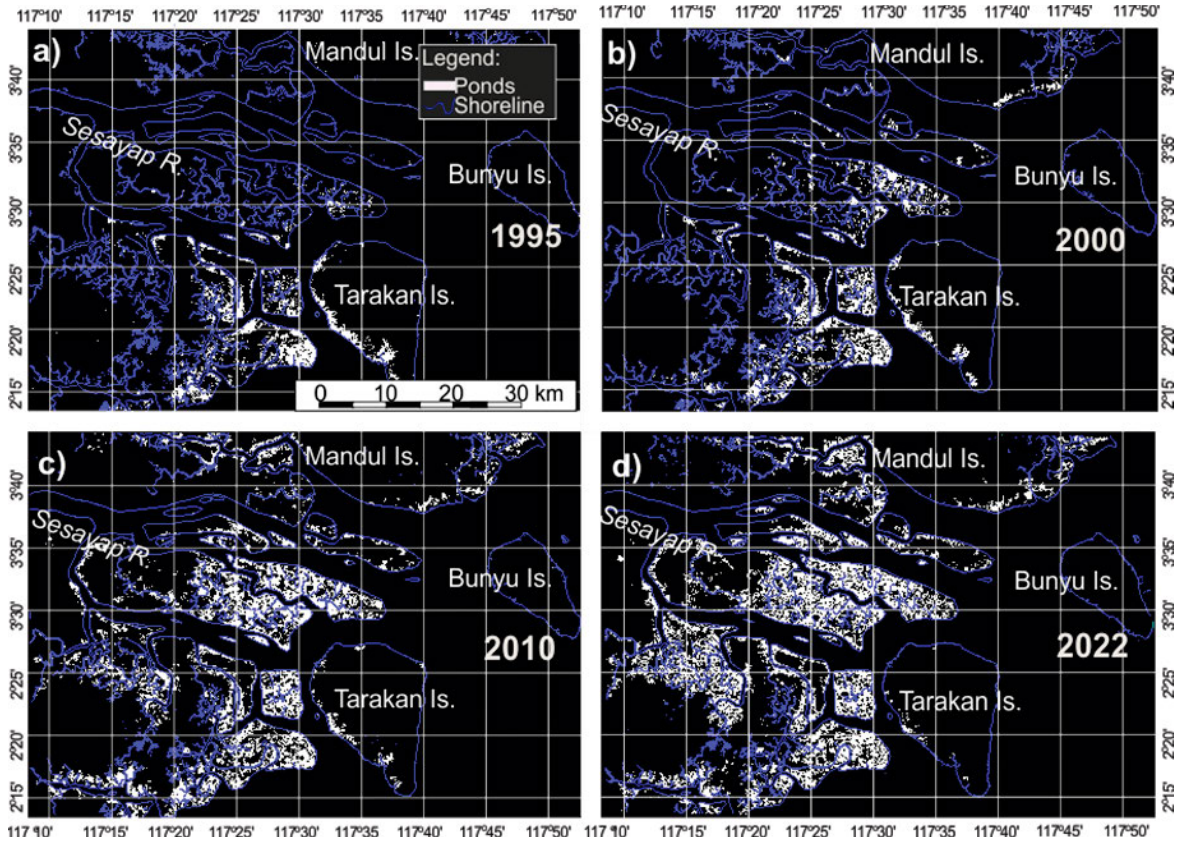

Fig. 5. Ponds encroachment in the study area from 1995 to 2022 in the north area of the Sesayap River Delta; Is. = island; source: own study

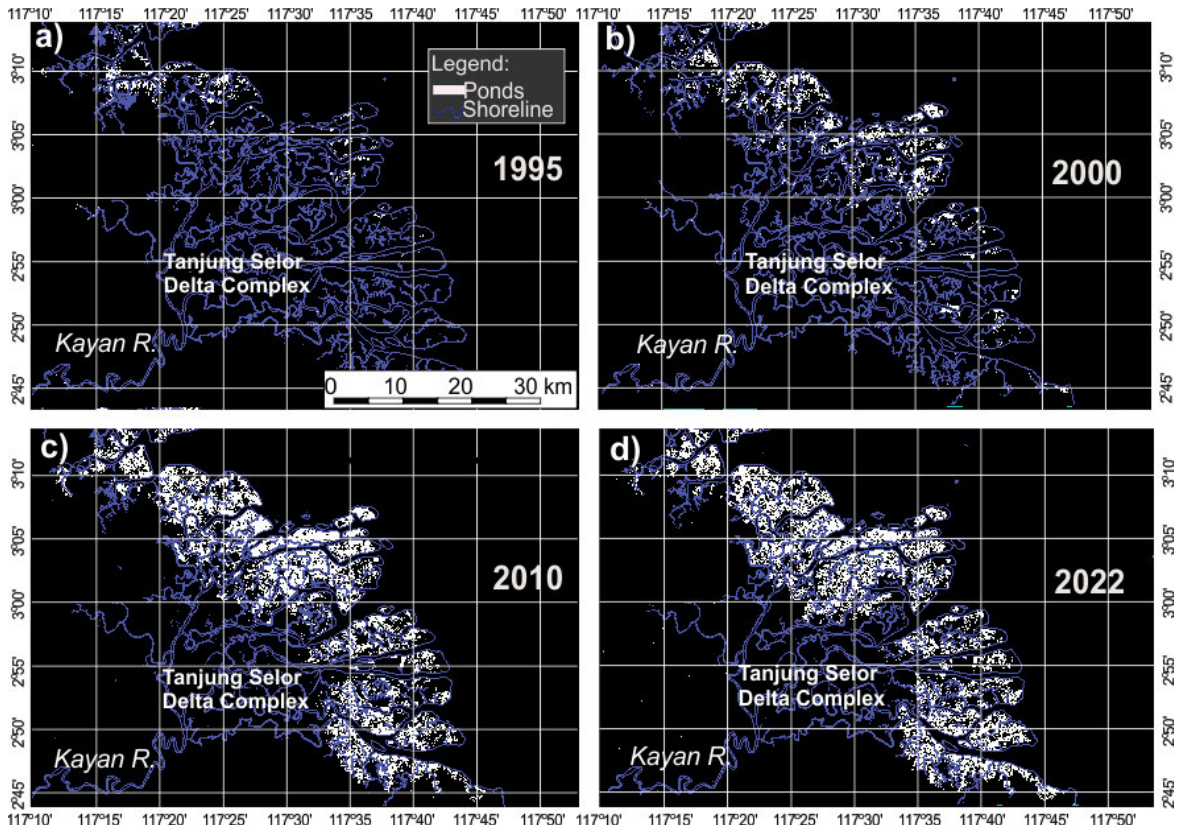

Fig. 6. Ponds encroachment in the study area from 1995 to 2022 in the south area of the Kayan River Delta; R. = river; source: own study

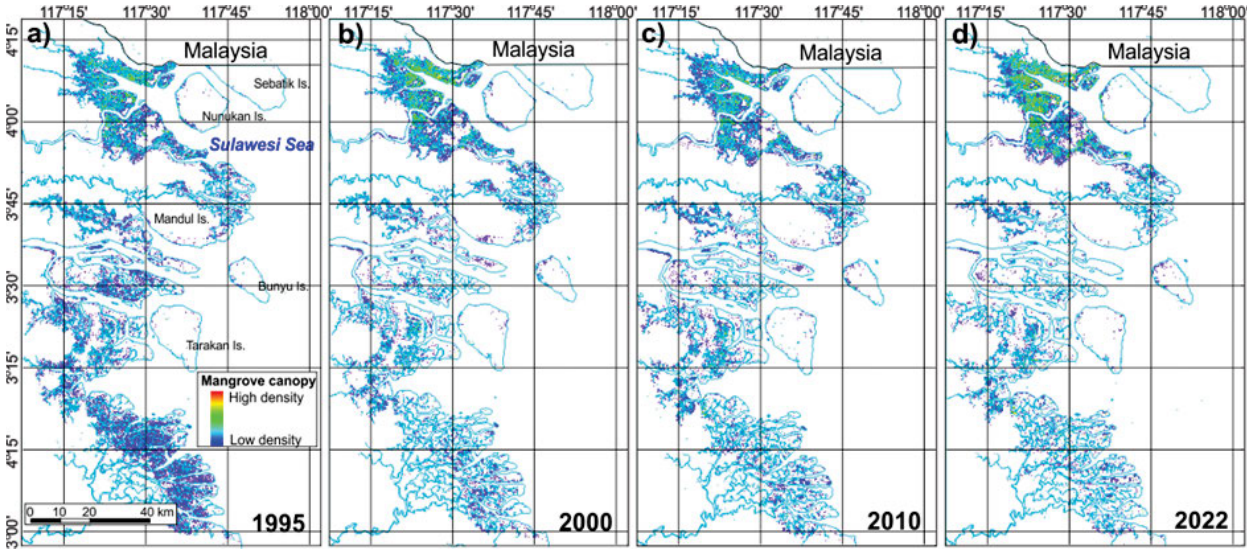

Fig. 7. Changes of mangroves in the study area from 1995 to 2022: a) 1995, b) 2000, c) 2010, d) 2022; Is. = island; source: own study

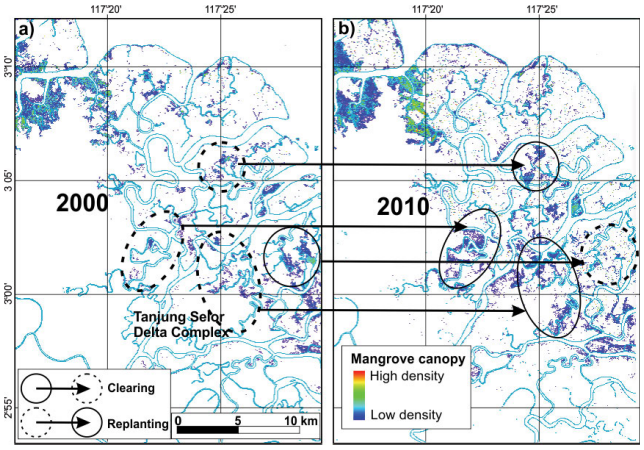

Fig. 8. Changes of mangroves in ponds environment in the Kayan River Delta/Tanjung Selor Delta complex in: a) 2000, b) 2010; source: own study

The 2022 Landsat 8 OLI image informs of the state of ponds and mangroves in 2022. The state of mangroves in 2022 is slightly different from the condition in 2010 with an expansion, while ponds are still being expanded (Figs. 5 and 6), although new ponds are not always opened in mangrove forest areas. Evidence shows that the mangrove area has continued to increase compared to 2010, including in former ponds that were previously opened (Figs. 7 and 8). The mangrove area in 2022 in the study area reaches 108,187 ha, while the pond area will increase to 84,182 ha (Tab. 5).

Table 5. Changes in mangrove and ponds growth in 1995–2022

Year	Mangrove	Ponds
	ha	
1995	150,869	14,456
2000	100,016	27,903
2010	106,867	74,270
2022	108,187	84,182

Source: own study.

FACTORS INFLUENCING MANGROVE DEGRADATION

The status of natural mangrove forests with few of ponds in the study area began in 1995 through analysis of 1995 Landsat TM imagery. The results of the analysis show that the northern part is an estuarine environment with little sedimentation from land in waters semi-enclosed by Sebatik Island and Nunukan Island, while the southern part is a delta environment of the Sesayap and Kayan rivers. Worthington *et al.* (2020) conducted a study which found that estuarine mangroves suffered relatively little damage, except from overexploitation. In contrast, delta mangroves are more susceptible to damage from dense population and land conversion, and even the Kayan and Sesayap deltas in Indonesia are reviewed in their paper as examples.

The economic crises in Indonesia in 1997–2000 were characterised by a decline in the economic situation due to the devaluation of the Indonesian currency (rupiah) against the US dollar. Inflation is a consequence of an ongoing economic crisis. The currency crisis was part of the Asian financial crisis, which was caused by a combination of inappropriate financial market behaviour and weak government policies. The devaluation of Thailand's currency (bath) against the US dollar spread to neighbouring countries in Southeast Asia. When the rupiah weakened against the US dollar, the demand for US dollars increased and the supply of dollars decreased. In January 1998, the rupiah exchange rate weakened from 4,850 to 13,600 per US dollar, peaking at 17,000 per US dollar. Local communities and entrepreneurs were attempting to produce export goods to generate US dollars. Shrimp exports are among the most promising exports. To realise this business, several coastal areas were encroached and new ponds were created. Pond areas that are considered potentially suitable are mostly located in coastal areas close to the coast and protected from coastal erosion processes. The chosen environment is usually a healthy mangrove area (Richards and Friess, 2015). This is a common practice among people in Southeast Asian countries such as Vietnam (Hauser *et al.*, 2017), Myanmar (Alban de *et al.*, 2020), Thailand (Macintosh, Ashtona and Havanon, 2002), and China (Chen *et al.*, 2009). Adame *et al.* (2018) and Gandhi and Jones (2019) also expressed the same opinion. The relationship between

mangrove destruction, fish pond expansion and the currency crisis is shown in Figure 9.

Mangroves in Indonesia are partly managed by the government and partly by the community. Community-managed mangroves are fragile and can be easily cut down because of a lack of oversight. The low index of the mangrove canopy in the Kahayan Delta in 1995 was believed to be caused by the dynamics of water level changes in the mangrove environment due to sedimentation processes in the delta, making ecological and hydrological conditions no longer suitable for mangrove growth and development as highlighted by Lewis (2005), Lewis and Brown (2014), Lee *et al.* (2019), and Lewis *et al.* (2019) (as cited in Long *et al.* (2022)). However, the Head of the Peat and Mangrove Restoration Authority of the Republic of Indonesia, in North Kalimantan introduced the policy of silvo-fishery (fishery business by planting mangroves) to allow people to manage their ponds and replant mangroves simultaneously (Asmalyah, 2022). The result shows that the mangroves have been able to survive and show a slight increase in area and canopy index since 2010. Such a remediation model, considering preserved water levels (in abandoned and unproductive ponds), can be used as a reference for other mangrove areas in need of remediation.

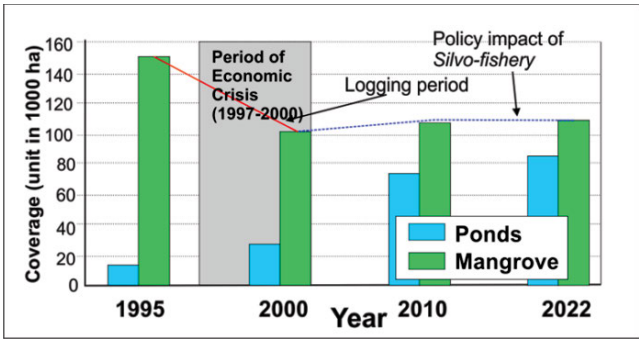

Fig. 9. Changes of ponds and mangroves from 1995 to 2022 in North Kalimantan; source: own study

CONCLUSIONS

Changes in mangroves converted to ponds were analysed based on multitemporal data from Landsat 5 TM in 1995, Landsat ETM 7 in 2000, Landsat ETM 7 in 2010, and Landsat 8 OLI in 2022. Landsat 5 TM imagery from 1995 shows that mangrove forests in North Kalimantan still look pristine and have some ponded areas. However, in the following period, ponds that had developed in the outer parts of the Sesayap and Kayan Delta grew further upstream and occupied a large part of the mangrove forest.

The economic crisis of 1997–1998 had a significant impact, as most mangrove areas, especially in the Sesayap and Kayan river deltas, were converted to ponds. However, the positive for the future in maintaining mangroves is that the silvo-fishery policy provided many valuable lessons on how to create ponds and reforest mangroves simultaneously. The results achieved include an increase in the mangrove area and an increase in the mangrove canopy index since 2010.

Mangrove degradation and pond encroachment are much faster than available mangrove data and maps. To respond to this situation, a combination of *AMMI* and *ASM* indices that are very easy to apply, low cost, faster, more efficient and accurate in producing mangrove maps and pond maps can be used as an alternative for better monitoring and management of mangrove environments.

ACKNOWLEDGEMENTS

This work is part of developing skills to increase human resources for monitoring mangrove health. The authors thank all colleagues at the Marine Geospatial Laboratory at the Research Center for Oceanography, National Research and Innovation Agency (BRIN), for providing the infrastructure to prepare this manuscript.

CONFLICT OF INTERESTS

All authors declare that they have no conflict of interests.

REFERENCES

Adame, M.F. *et al.* (2018) "The undervalued contribution of mangrove protection in Mexico to carbon emission targets," *Conservation Letters*, 11(4), e12445. Available at: https://doi.org/10.1111/conl.12445.

Alban de, J.D.T. *et al.* (2020) "Improved estimates of mangrove cover and change reveal catastrophic deforestation in Myanmar," *Environmental Research Letters*, 15(3), 034034. Available at: https://doi.org/10.1088/1748-9326/ab666d.

Alongi, D.M. (2002) "Present state and future of the world's mangrove forests," *Environmental Conservation*, 29(3), pp. 331–349. Available at: https://doi.org/10.1017/S0376892902000231.

Asmalyah, S. (2022) *BRGM bakal terapkan "silvofishery" mangrove di Kalimantan Utara [The Peat and Mangrove Restoration Agency (BRGM) implement mangrove silvofishery in North Kalimantan]. Antara*. Available at: https://www.antaranews.com/berita/3255405/brgm-bakal-terapkan-silvofishery-mangrove-di-kalimantan-utara (Accessed: May 21, 2023).

BIG (2017) *Peta Rupabumi Indonesia skala 1:250.000 [Indonesian Topographic Map, scale: 1:250.000]*. Cibinong: Badan Informasi Geospasial.

Boon, J.M. (2001) "A socio-economic analysis of mangrove degradation in Samoa," *Geographical Review of Japan, Series B*, 74(2), pp. 159–186. Available at: https://doi.org/10.4157/grj1984b.74.159.

Brooks, N. (2003) *Vulnerability, risk, and adaptation: A conceptual framework*, Norwich: Tyndall Centre for Climate Change Research, University of East Anglia.

Chen, L. *et al.* (2009) "Recent progresses in mangrove conservation, restoration and research in China," *Journal of Plant Ecology*, 2(2), pp. 45–54. Available at: https://doi.org/10.1093/jpe/rtp009.

Costanza, R. *et al.* (1997) "The value of the world's ecosystem services and natural capital," *Nature*, 387, pp. 253–260. Available at: https://doi.org/10.1038/387253a0.

Dahdouh-Guebas, F. *et al.* (2006) "How effective were mangroves as a defence against the recent tsunami?," *Current Biology*, 15(12), pp. 443–446. Available at: https://doi.org/10.1016/j.cub.2005.06.008.

Danielsen, F. *et al.* (2005) "The Asian tsunami: A protective role for coastal vegetation," *Science*, 310(5748), 643. Available at: https://doi.org/10.1126/science.1118387.

Das, S. and Vincent, J.R. (2009) "Mangroves protected villages and reduced the death toll during the Indian super cyclone," *Proceedings of the National Academy of Sciences USA*, 106(18), pp. 7357–7360. Available at: https://doi.org/10.1073/pnas.0810440106.

Ding, F. (2009) "Study on information extraction of water body with a new water index (NWI)," *Surveying and Mapping Science*, 34(4), pp. 155–157 [in Chinese].

Donato, D.C. *et al.* (2011) "Mangroves are among the most carbon-rich forests in the tropics," *Nature Geoscience*, 4(5) pp. 293–297. Available at: https://doi.org/10.1038/ngeo1123.

Duke, N.C. *et al.* (2007) "A world without mangroves?," *Science*, 317 (5834), pp. 41–42. Available at: https://doi.org/10.1126/science.317.5834.41b.

Fatoyinbo, T.E. *et al.* (2008) "Landscape-scale extent, height, biomass, and carbon estimation of Mozambique's mangrove, forests with Landsat ETM+, and Shuttle Radar Topography Mission elevation data," *Journal of Geophysical Research*, 113(2). Available at: https://doi.org/10.1029/2007JG000551.

Fisher, A., Flood, N. and Danaher, T. (2016) "Comparing Landsat water index methods for automated water classification in eastern Australia," *Remote Sensing of Environment*, 175, pp. 167–182. Available at: https://doi.org/10.1016/j.rse.2015.12.055.

Gandhi, S. and Jones, T.G. (2019) "Identifying mangrove deforestation hotspots in South Asia, Southeast Asia and Asia-Pacific," *Remote Sensing*, 11(6), 728. Available at: https://doi.org/10.3390/rs11060728.

Gilman, E.L. *et al.* (2008) "Threats to mangroves from climate change and adaptation options: a review," *Aquatic Botany*, 89, pp. 237–250. Available at: https://doi.org/10.1016/j.aquabot.2007.12.009.

Giri, C. *et al.* (2011) "Status and distribution of mangrove forests of the world using earth observation satellite data," *Global Ecology and Biogeography*, 20(1), pp. 154–159. Available at: https://doi.org/10.1111/j.1466-8238.2010.00584.x.

Gorelick, N. *et al.* (2017) "Google Earth engine: Planetary-scale geospatial analysis for everyone," *Remote Sensing of Environment*, 202, pp. 18–27. Available at: https://doi.org/10.1016/j.rse.2017.06.031.

Guo, X., *et al.* (2018) "Vegetation horizontal occlusion index (VHOI) from TLS and UAV image to better measure mangrove LAI," *Remote Sensing*, 10(11), 1739. Available at: https://doi.org/10.3390/rs10111739.

Hauser, L.T. *et al.* (2017) "Uncovering the spatio-temporal dynamics of land cover change and fragmentation of mangroves in the Ca Mau peninsula, Vietnam using multi-temporal SPOT satellite imagery (2004–2013)," *Applied Geography*, 86, pp. 197–207. Available at: https://doi.org/10.1016/j.apgeog.2017.06.019.

Huang, C. *et al.* (2018) "Detecting, extracting, and monitoring surface water from space using optical sensors: A review," *Reviews of Geophysics*, 56, pp. 333–360. Available at: https://doi.org/10.1029/2018RG000598.

Jones, A.R. *et al.* (2020) "Estimating mangrove tree biomass and carbon content: A comparison of forest inventory techniques and drone imagery," *Frontiers in Marine Science*, 6, 784. Available at: https://doi.org/10.3389/fmars.2019.00784.

Kanniah, K.D. *et al.* (2015) "Satellite images for monitoring mangrove cover changes in a fast growing economic region in Southern Peninsular Malaysia," *Remote Sensing*, **7**(11), pp. 14360–14385. Available at: https://doi.org/10.3390/rs71114360.

Kim, K. *et al.* (2016) "Novel water filtration of saline water in the outermost layer of mangrove roots," *Scientific Reports*, 6, 20426. Available at: https://doi.org/10.1038/srep20426.

Kuenzer, C. *et al.* (2011) "Remote sensing of mangrove ecosystems: A review," *Remote Sensing*, 3(5), pp. 878–928. Available at: https://doi.org/10.3390/rs3050878.

Li, J. *et al.* (2022) "Satellite detection of surface water extent: A review of methodology," *Water*, *14(7),* 1148. Available at: https://doi.org/10.3390/w14071148.

Long, C. *et al.* (2022) "Dynamic changes in mangroves of the largest delta in northern Beibu Gulf, China: Reasons and causes," *Forest Ecology and Management*, 504, 119855. Available at: https://doi.org/10.1016/j.foreco.2021.119855.

Macintosh, D.J., Ashtona, E.C. and Havanon, S. (2002) "Mangrove rehabilitation and intertidal biodiversity: A study in the Ranong Mangrove Ecosystem, Thailand," *Estuarine, Coastal and Shelf Science*, 55, pp. 331–345. Available at: https://doi.org/10.1006/ECSS.2001.0896.

McFeeters, S.K. (1996) "The use of the normalized difference water index (NDWI) in the delineation of open water features," *International Journal of Remote Sensing*, 17, pp. 1425–1432. Available at: https://doi.org/10.1080/01431169608948714.

Nagelkerken, I. *et al.* (2008) "The habitat function of mangroves for terrestrial and marine fauna: A review," *Aquatic Botany*, 89(2), pp. 155–185. Available at: https://doi.org/10.1016/j.aquabot.2007.12.007.

Ng, C.K-C. and Ong, R.C. (2022) "A review of anthropogenic interaction and impact characteristics of the Sundaic mangroves in Southeast Asia," *Estuarine. Coastal and Shelf Science*, 267, 107759. Available at: https://doi.org/10.1016/j.ecss.2022.107759.

Purnamasayangsukasih, P.R. *et al.* (2016) "A review of uses of satellite imagery in monitoring mangrove forests," *IOP Conference Series: Earth and Environmental Science*, 37, 012034. Available at: https://doi.org/10.1088/1755-1315/37/1/012034.

Richards, D.R. and Friess, D.A. (2015) "Rates and drivers of mangrove deforestation in Southeast Asia, 2000–2012," *Proceedings of the National Academy of Sciences*, 113(2), pp. 344–349. Available at: https://doi.org/10.1073/pnas.1510272113.

Ross, M.S. *et al.* (2006) "Early post-hurricane stand development in Fringe mangrove forests of contrasting productivity," *Plant Ecology*, 185(2), pp. 283–297. Available at: https://doi.org/10.1007/s11258-006-9104-9.

Sanderman, J. *et al.* (2018) "A global map of mangrove forest soil carbon at 30 m spatial resolution," *Environmental Research Letters*, 13(5), 055002. Available at: https://doi.org/10.1088/1748-9326/aabe1c.

Shen, L. and Li, C. (2010) "Water body extraction from Landsat ETM+ imagery using adaboost algorithm," *18th International Conference on Geoinformatics*, pp. 1–4. Available at: https://doi.org/10.1109/GEOINFORMATICS.2010.5567762.

Sierra-Correa, P.C. and Kintz, J.R.C. (2015) "Ecosystem-based adaptation for improving coastal planning for sea-level rise: A systematic review for mangrove coasts," *Marine Policy*, 51, pp. 385–393. Available at: https://doi.org/10.1016/j.marpol.2014.09.013.

Soemodihardjo, S., Suroyo and Suyarso (1991) "The mangrove forest of Segara Anakan: An assessment of their condition and prospect," in L.M. Chou *et al.* (eds.) *Towards an integrated management of tropical coastal resources, Proceedings of the ASEAN/US technical workshop on integrated tropical coastal zone management*, pp. 213–222, Singapore, 28–31 Oct 1988. Singapore: National University of Singapore.

Suyarso (2022) "AMMI Automatic Mangrove Map and Index: An analytical study on satellite imageries at Aru Islands, Maluku,

Indonesia," *Emerging Challenges in Environment and Earth Science*, 2, pp. 106–130. Available at: https://doi.org/10.9734/bpi/ecees/v2/3423e.

Suyarso and Avianto, P. (2022) "AMMI Automatic Mangrove Map and Index: Novelty for efficiently monitoring mangrove changes with the case study in Musi Delta, South Sumatra, Indonesia," *International Journal of Forestry Research*, 2022, 8103242. Available at: https://doi.org/10.1155/2022/8103242.

Taylor, M.D.M.R.B., Rangel-Salazar, J.L. and Hernández, B.C. (2013) "Resilience in a Mexican Pacific mangrove after hurricanes: Implications for conservation-restoration," *Journal of Environmental Protection*, 4, pp. 1383–1391. Available at: https://doi.org/10.4236/jep.2013.412159.

Thakur, S. *et al.* (2020) "A review of the application of multispectral remote sensing in the study of mangrove ecosystems with special emphasis on image processing techniques," *Spatial Information Research*, 28(1), pp. 39–51. Available at: https://doi.org/10.1007/s41324-019-00268-y.

Thu, P.M. and Populus, J. (2007) "Status and changes of mangrove forest in Mekong Delta: Case study in Tra Vinh, Vietnam," *Estuarine Coastal and Shelf Science*, 71(1–2), pp. 98–109. Available at: https://doi.org/10.1016/j.ecss.2006.08.007.

USGS (no date) *What are the band designations for the Landsat satellites?* USGS science for changing world. Available at: https://www.usgs.gov/faqs/what-are-band-designations-landsat-satellites (Accessed: May 21, 2023).

Valiela, I., Bowen, J.L. and York, J.K. (2001) "Mangrove forests: One of the world's threatened major tropical environments," *Bioscience*, 51(10), pp. 807–815. Available at: https://doi.org/10.1641/0006-3568(2001)051[0807:MFOOTW]2.0.CO;2.

Veettil, B.K. *et al.* (2018) "Mangroves of Vietnam: Historical development, current state of research and future threats," *Estuarine Coastal and Shelf Science*, 218, pp. 212–236. Available at: https://doi.org/10.1016/j.ecss.2018.12.021.

Wang, L. *et al.* (2019) "A review of remote sensing for mangrove forests: 1956–2018," *Remote Sensing of Environment*, 231, 111223. Available at: https://doi.org/10.1016/j.rse.2019.111223.

Wang, M. *et al.* (2010) "Maintenance of estuarine water quality by mangroves occurs during flood periods: A case study of a subtropical mangrove wetland," *Marine Pollution Bulletin*, 60(11), pp. 2154–2160. Available at: https://doi.org/10.1016/j.marpolbul.2010.07.025.

Wang, X. *et al.* (2018) "A robust Multi-Band Water Index (MBWI) for automated extraction of surface water from Landsat 8 OLI imagery," *International Journal of Applied Earth Observation and Geoinformation*, 68, pp. 73–91. Available at: https://doi.org/10.1016/j.jag.2018.01.018.

Wicaksono, P. *et al.* (2016) "Mangrove biomass carbon stock mapping of the Karimunjawa Islands using multispectral remote sensing," *International Journal of Remote Sensing*, 37(1), pp. 26–52. Available at: https://doi.org/10.1080/01431161.2015.1117679.

Wong, Y.S., Tam, N.F.Y. and Lan, C.Y. (1997) "Mangrove wetlands as a wastewater treatment facility: A field trial," *Hydrobiologia*, 352 (1/3), pp. 49–59. Available at: https://doi.org/10.1023/a:1003040920173.

Worthington, T.A. *et al.* (2020) "A global biophysical typology of mangroves and its relevance for ecosystem structure and deforestation," *Scientific Reports*, 10(1). Available at: https://doi.org/10.1038/s41598-020-71194-5.

Xu, H. (2006) "Modification of normalised difference water index (NDWI) to enhance open water features in remotely sensed imagery," *International Journal of Remote Sensing*, 27(14), pp. 3025–3033. Available at: https://doi.org/10.1080/01431160600589179.

Yam, R.S.W. *et al.* (2020) "Assessing impacts of metallic contamination along the tidal gradient of a riverine mangrove: Multi-metal Bioaccumulation and biomagnification of filter-feeding bivalves," *Forests*, 11(5), 504. Available at: https://doi.org/10.3390/f11050504.